RNA (1997), 3:893–904. Cambridge University Press. Printed in the USA.

Structure and aminoacylation capacities of tRNA transcripts containing deoxyribonucleotides

RUSLAN APHASIZHEV,[1,2,3] ANNE THÉOBALD-DIETRICH,[1] DMITRY KOSTYUK,[2] SERGEY N. KOCHETKOV,[2] LEV KISSELEV,[2] RICHARD GIEGÉ,[1] and FRANCO FASIOLO[1]

[1]UPR 9002, IBMC du CNRS, 15 rue René Descartes, F-67084 Strasbourg Cedex, France
[2]Engelhardt Institute of Molecular Biology, Vavilov Street 32, Moscow 117984, Russia

ABSTRACT

The contribution of the ribose 2′-hydroxyls to RNA structure and function has been analyzed, but still remains controversial. In this work, we report the use of a mutant T7 RNA polymerase as a tool in RNA studies, applied to the aspartate and methionine tRNA aminoacylation systems from yeast. Our approach consists of determining the effect of substituting natural ribonucleotides by deoxyribonucleotides in RNA and, thereby, defining the subset of important 2′-hydroxyl groups. We show that deoxyribose-containing RNA can be folded in a global conformation similar to that of natural RNA. Melting curves of tRNAs, obtained by temperature-gradient gel electrophoresis, indicate that in deoxyribo-containing molecules, the thermal stability of the tertiary network drops down, whereas the stability of the secondary structure remains unaltered. Nuclease footprinting reveals a significant increase in the accessibility of both single- and double-stranded regions.

As to the functionality of the deoxyribose-containing tRNAs, their in vitro aminoacylation efficiency indicates striking differential effects depending upon the nature of the substituted ribonucleotides. Strongest decrease in charging occurs for yeast initiator $tRNA^{Met}$ transcripts containing dG or dC residues and for yeast $tRNA^{Asp}$ transcripts with dU or dG. In the aspartate system, the decreased aminoacylation capacities can be correlated with the substitution of the ribose moieties of U11 and G27, disrupting two hydrogen bond contacts with the synthetase. Altogether, this suggests that specific 2′-hydroxyl groups in tRNAs can act as determinants specifying aminoacylation identity.

Keywords: aspartyl-tRNA synthetase; deoxyribonucleotide-containing RNAs; methionyl-tRNA synthetase; mutant T7 RNA polymerase; structural probing; temperature gradient gel electrophoresis (TGGE)

INTRODUCTION

Searching for functionally and structurally important chemical groups in RNA, three targets exist: the nucleotide bases, the sugar, and the phosphate moieties. Historically, the focus was on the contribution of specific bases to RNA structure and function. Recent advances in RNA modification techniques have yielded an impressive progress in the understanding of the role of sugar–phosphate moiety. Functional studies of 2′-hydroxyls are rather modest in number and mostly concern the ribozyme catalysis (Pyle & Cech, 1991; Pyle et al., 1992; Williams et al., 1992). For tRNAs, the contacts of 2′-OH groups with proteins became evident from high-resolution crystal structure of tRNA/aminoacyl-tRNA synthetase complexes (Rould et al., 1989; Cavarelli et al., 1993; Biou et al., 1994). Biochemical analyses using oligonucleotides synthesized chemically revealed the contribution of particular 2′-OH in binding affinity for $tRNA^{Ala}$-based minihelices to alanyl-tRNA synthetase (Musier-Forsyth & Schimmel, 1992). The critical interaction of a 2′-OH with a base for aminoacylation in *Escherichia coli* $tRNA^{Pro}$ has been identified recently (Yap & Musier-Forsyth, 1995). Earlier aminoacylation activity data on chemically synthesized *E. coli* $tDNA^{Phe}$ (Khan & Roe, 1988) and nuclease probing of *E. coli* $tDNA^{Met}$ structure in solution (Paquette et al., 1990) demonstrated that the ribose–phosphate backbone of tRNA is not absolutely required for maintaining the tRNA structure and function.

The apparent ambiguity of the existing information prompted us to continue the elucidation of the role of 2′-OH in tRNA. Routine RNA phosphoramide synthesis is still limited to 40–50 nt, even though many RNAs are longer. The elegant approach for introduction of specific 2′-OH modifications in long RNAs (pre-mRNAs, for instance) has been proposed by Moore and Sharp (1992). It explores ligation of segments by

Reprint requests to: R. Giegé and F. Fasiolo, UPR 9002, IBMC du CNRS, 15 rue René Descartes, F-67084 Strasbourg Cedex, France.
[3]Present address: Howard Hughes Medical Institute, University of California, Los Angeles, California 90095-1662, USA.

the T4 DNA ligase, one of which contains the desired modification at the 5′ end. Another way to obtain 2′-modified RNAs relies on enzymatic transcription of the corresponding DNA templates with T7 phage RNA polymerase using 2′-modified (Aurup et al., 1992) or deoxy- (Conrad et al., 1995) nucleotides. In the last case, the conversion of RNA polymerase to DNA polymerase has been achieved by using Mn^{2+} instead of Mg^{2+} in the reaction mixture. However, apparently not all deoxyribonucleotides could be incorporated into transcripts by this method.

Recently, we (Kostyuk et al., 1995) and others (Sousa & Padilla, 1995) have described the engineering of T7 RNA polymerase mutants that are able to incorporate deoxyribonucleotides into RNA. Here we report the application of this mutant T7 polymerase as a tool in RNA research. Our approach consists of determining the deoxyribonucleotide substitution effects on RNA structure and function and, thereby, defining the subset of important 2′-OH groups. It was applied to tRNA transcripts of aspartate and methionine specificities for several reasons: (1) transcripts of tRNA, contrary to all natural (mature) RNAs, are devoid of modified nucleotides that may interfere with the properties of deoxyribo-substituted molecules; (2) the three-dimensional (3D) structure tRNA is known and correlations between structural and functional features are rather well characterized (reviewed in Giegé et al., 1993); (3) the 3D structure of the complex between a synthetase and its tRNA substrate is established for the aspartate pair (Ruff et al., 1991; Cavarelli et al., 1993); (4) the molecules are relatively short, enabling the direct analysis of substitutions in the nucleotide sequences; and (5) a straightforward functional testing (the aminoacylation capacity) is available.

RESULTS

Incorporation of 2′-deoxyribonucleotides into $tRNA^{Asp}$ and $tRNA^{Met}$ transcripts with a mutant T7 RNA polymerase

Sequences of the two tRNA transcripts of this study are shown in Figure 1A. Specificity of template-dependent incorporation was determined by alkaline treatment of 5′-labeled $tRNA^{Met}$ followed by sequence analysis (Fig. 1B,C). Gaps in alkaline ladders indicate the occurrence of deoxyribonucleotides in the sequence. When Mg^{2+} was added to the transcription buffer, no background bands were seen in the gaps corresponding to deoxyribonucleotide positions. Therefore, we concluded that the mutant T7 RNA polymerase remains completely specific in terms of base pairing between DNA template and RNA product.

In previous studies on conversion of RNA to DNA polymerases, it was noted that the efficiency of incorporation of a particular deoxyribonucleotide depends on its distance from the 5′ end of the RNA transcript (Sousa & Padilla, 1995). Figure 2 shows the relative yield of full-length tRNA transcripts, synthesized with one or two deoxyribonucleotide(s), and purified by denaturing gel electrophoresis. Analysis of the transcription efficiency indicates that the later the first deoxyribonucleotide is added to the growing RNA transcript, the more efficient the transcription proceeds. We were able to achieve the incorporation of two dNTPs only for dAdU $tRNA^{Met}$, whereas all other double combinations for both $tRNA^{Met}$ and $tRNA^{Asp}$ failed to produce sufficient amounts of RNA transcripts for further analysis.

To improve the yield of transcription, we tried a Mn^{2+}-containing buffer that reduces discrimination between ribo- and deoxyribonucleotides for many polymerases, including that of phage T7 (Conrad et al., 1995). However, RNAs obtained in that way contained up to 10% of unspecific incorporation (not shown) and, therefore, were considered unsuitable for further analysis.

It was particularly interesting to reveal whether the mutant polymerase is able to incorporate at once ribo- and deoxyribonucleotides at the same position in the transcript if both triphosphate derivatives were present in the reaction mixture. Such a hybrid molecule can then be a subject for modification interference studies. Figure 1C shows that dU/rU-containing transcript may actually be synthesized. However, relative incorporation is not exactly proportional to the relative concentrations of ribo- and deoxyribonucleotide in the reaction mixture. The reason for this effect is not clearly understood yet, and could be linked to context effects brought about by particular RNA sequences.

Overall conformation of $tRNA^{Asp}$ and $tRNA^{Met}$ transcripts containing 2′-deoxyribonucleotides

To assess whether the global folding of tRNA transcripts containing deoxyribonucleotides is preserved, we applied native gel electrophoresis, shown to be sensitive to the overall tRNA conformation (Yap & Musier-Forsyth, 1995). One-nucleotide-substituted $tRNA^{Met}$ transcripts were compared, after a renaturation step, with samples that had not been renatured (Fig. 3A). Without renaturation, the tRNA transcripts run as two major bands, indicating the presence of at least two conformers, which could be separated in nondenaturing conditions. The renaturation procedure converted transcripts into a single conformer that had the same mobility as the lower band in the nontreated samples and presumably corresponded to the folded RNA. For $tRNA^{Asp}$ (Fig. 3B), the differences in mobility between folded and unfolded states were insignificant. In this case, we run a three times longer gel to visualize the difference. From these results we assume that deoxyribonucleotide-containing tRNA transcripts

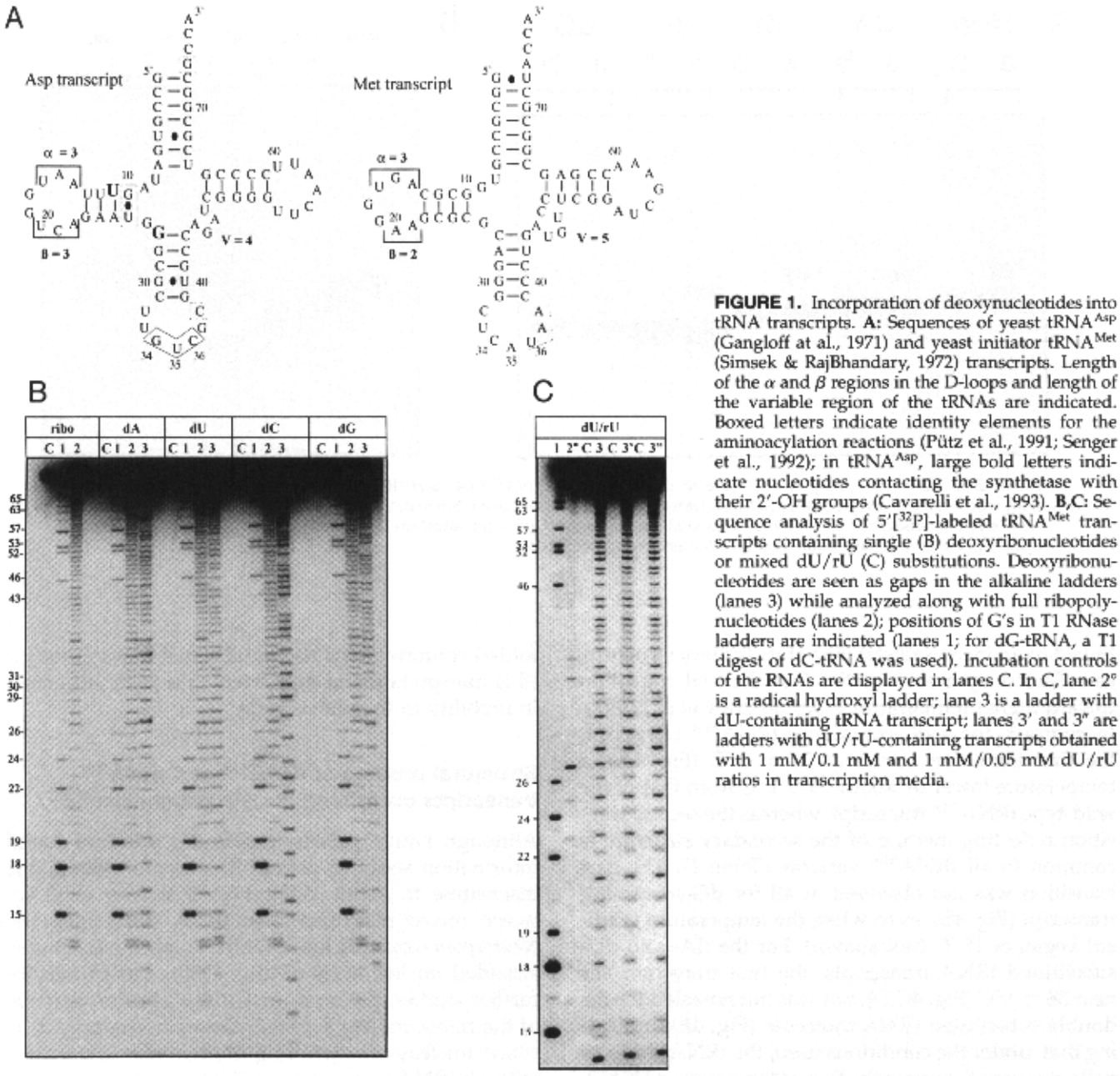

FIGURE 1. Incorporation of deoxynucleotides into tRNA transcripts. **A:** Sequences of yeast $tRNA^{Asp}$ (Gangloff at al., 1971) and yeast initiator $tRNA^{Met}$ (Simsek & RajBhandary, 1972) transcripts. Length of the α and β regions in the D-loops and length of the variable region of the tRNAs are indicated. Boxed letters indicate identity elements for the aminoacylation reactions (Pütz et al., 1991; Senger et al., 1992); in $tRNA^{Asp}$, large bold letters indicate nucleotides contacting the synthetase with their 2'-OH groups (Cavarelli et al., 1993). **B,C:** Sequence analysis of 5'-[^{32}P]-labeled $tRNA^{Met}$ transcripts containing single (B) deoxyribonucleotides or mixed dU/rU (C) substitutions. Deoxyribonucleotides are seen as gaps in the alkaline ladders (lanes 3) while analyzed along with full ribopolynucleotides (lanes 2); positions of G's in T1 RNase ladders are indicated (lanes 1; for dG-tRNA, a T1 digest of dC-tRNA was used). Incubation controls of the RNAs are displayed in lanes C. In C, lane 2° is a radical hydroxyl ladder; lane 3 is a ladder with dU-containing tRNA transcript; lanes 3' and 3" are ladders with dU/rU-containing transcripts obtained with 1 mM/0.1 mM and 1 mM/0.05 mM dU/rU ratios in transcription media.

may possess the global conformation of the corresponding full-ribo transcripts.

To define whether the stability of tertiary or secondary structure, or both, was affected by deoxyribo-substitution, melting experiments using temperature-gradient gel electrophoresis (TGGE) were performed. In this method, RNA conformational transitions are visualized by a change in the slope of migration due to the lower electrophoretic mobility of denatured molecules when a temperature gradient is applied perpendicularly to the direction of migration of the RNA molecules (Riesner et al., 1991). This method was applied to the analysis of a $tRNA^{Met}$ tertiary mutant and it could be shown that the k_{cat} defect of this mutant is

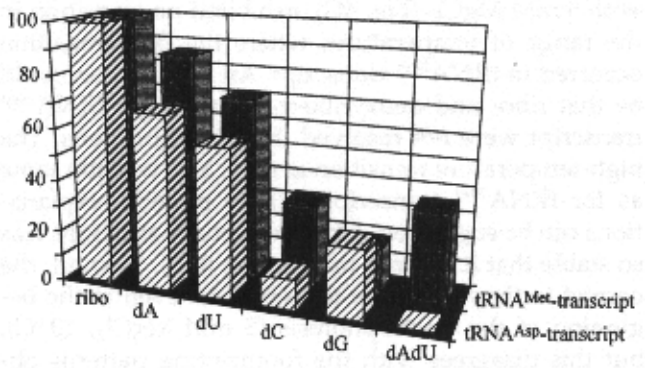

FIGURE 2. Relative yields of transcriptions for full-length deoxyribonucleotide-substituted tRNA transcripts.

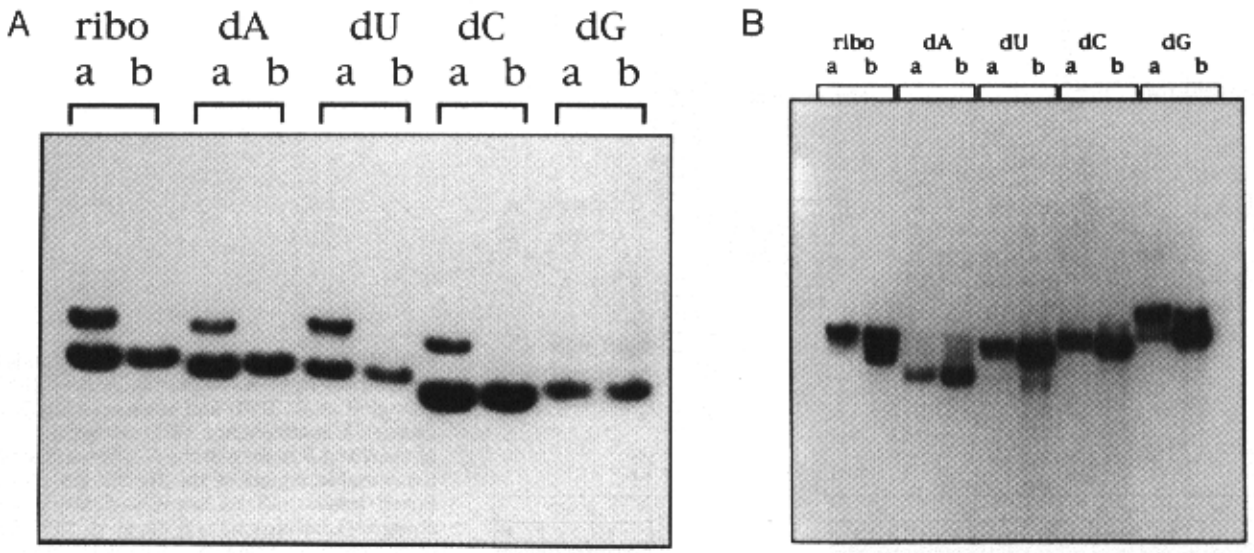

FIGURE 3. Native gel analysis of 5′-labeled dN-containing $tRNA^{Met}$ (**A**) and $tRNA^{Asp}$ (**B**) transcripts and comparison with wild-type transcripts. Lanes a, tRNA transcripts electroeluted from denaturing gels containing 8 M urea, precipitated with ethanol, dissolved in water, and loaded on the native gel after addition of glycerol up to 10%; lanes b, tRNA transcripts after a renaturation step (see Materials and Methods).

linked to an increased stability of its tertiary structure, as reflected by a shift of the first thermal transition toward higher temperatures (Aphasizhev et al., 1997). In contrast, for a dC-containing $tRNA^{Met}$ transcript, the first transition occurs at 32 ± 2 °C (Fig. 4A), a temperature lower by about 10 ± 1 °C from that of the wild-type $tRNA^{Met}$ transcript, whereas the second transition reflecting melting of the secondary structure is common to all $tRNA^{Met}$ variants (Table 1). The first transition was not observed at all for dG-containing transcript (Fig. 4B), even when the temperature gradient began at 15 °C (not shown). For the dA- and dU-substituted tRNA transcripts, the first transition lies near 38 ± 2 °C (Fig. 4C,D), but was not revealed for the double-substituted tRNA molecule (Fig. 4E), indicating that, under the conditions used, the tRNA was partially denatured, even at the lowest temperature (20 °C).

Melting curves of $tRNA^{Asp}$ and dG $tRNA^{Asp}$ transcripts, both in low ionic strength buffer (Fig. 4F) and with 5 mM $MgCl_2$ (Fig. 4G), exhibited no transition in the range of temperatures where the first transition occurred in $tRNA^{Met}$ transcript. An explanation could be that ribo- and deoxyribo-variants of the $tRNA^{Asp}$ transcript were not resolved in these conditions. The high-temperature transition at 65 ± 1 °C was the same as for $tRNA^{Met}$ transcripts. Three possible explanations can be suggested. First, the tertiary structure was so stable that it did not melt before 65 °C. Second, the correct tertiary structure did not exist even at the beginning of the electrophoresis (5 mM $MgCl_2$, 10 °C), but this disagrees with the footprinting patterns obtained in the same salt conditions (Perret et al., 1990b). Third and more likely, the partially denatured and folded conformations had similar mobilities in the gel (this interpretation is supported by a small difference in mobility in the native gel).

Structural probing of $tRNA^{Asp}$ and $tRNA^{Met}$ transcripts containing 2′-deoxyribonucleotides

Although native gel electrophoresis provides useful information about an overall RNA conformation, it is insensitive to subtle differences that may exist between mixed ribo/deoxyribo tRNA transcripts. The *Neurospora crassa* nuclease, which is specific for single-stranded nucleic acids (Fraser, 1980), was chosen for further studies, due to its insensitivity to the structure of the ribose moiety. Figure 5 shows an example of *N. crassa* nuclease footprinting experiments performed with all tRNA transcripts available so far.

The cleavage patterns displayed in the tRNA cloverleaf structures are shown in Figure 6. At first glance, it appears clearly from the number and strength of cuts (visualized by a color code) that both the substituted $tRNA^{Met}$ and $tRNA^{Asp}$ transcripts are more susceptible to nuclease cleavage than the wild-type molecules.

Wild-type $tRNA^{Met}$ transcript has a strong cut at position 58, and cuts at positions 17, 19, and 47 are also clearly visible; minor cuts are at positions 20, 34, and 36 (Fig. 6A). To some extent, the digestion patterns reflect the folding of tRNA: cuts in the loop regions correspond to nucleotides that do not participate in tertiary interactions. The anticodon loop of $tRNA^{Met}$ from *E. coli* is highly resistant to nucleases (Seong & RajBhandary, 1987), and it turns out to be the same for yeast $tRNA^{Met}$. The minor cuts may result from spon-

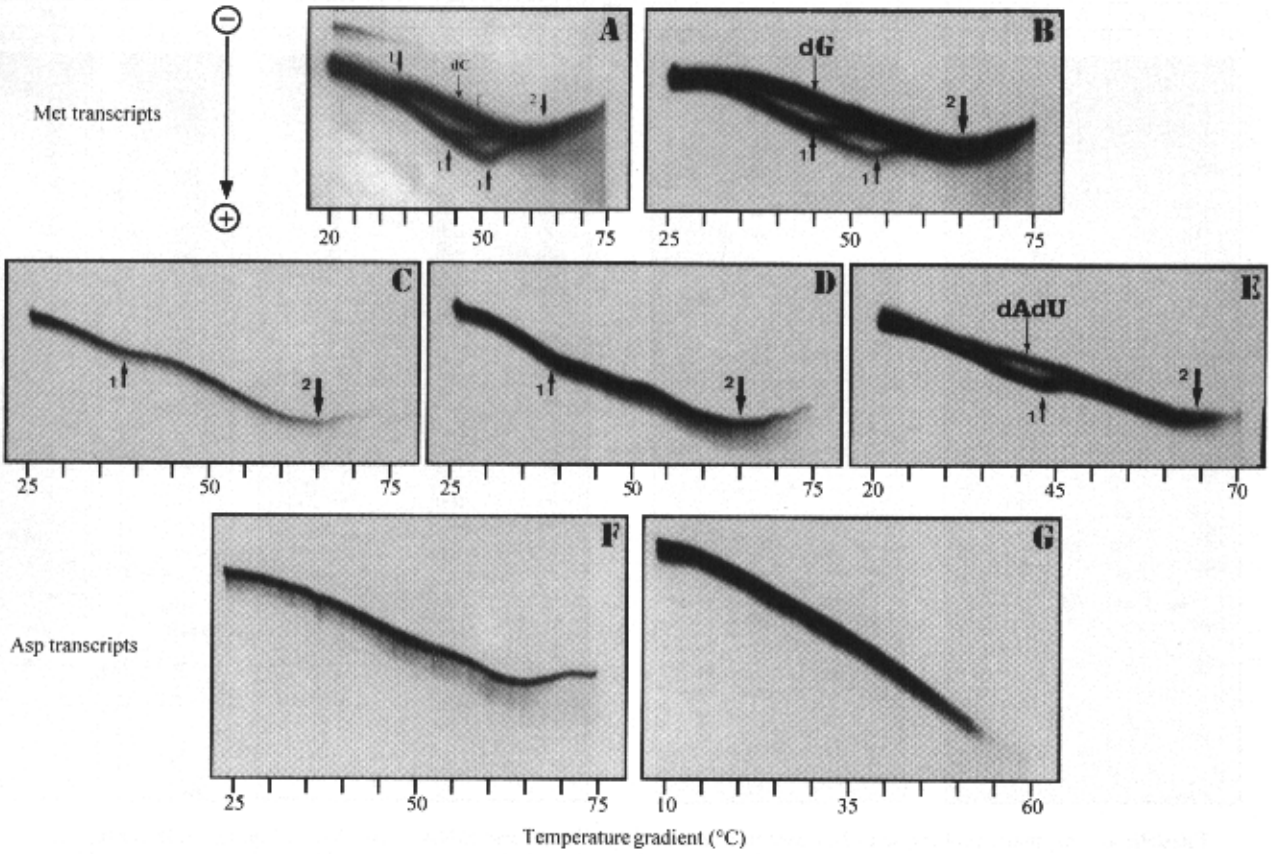

FIGURE 4. TGGE-melting profiles of deoxy-containing $tRNA^{Met}$ and $tRNA^{Asp}$ variants. First (1) and second (2) melting transition-points are indicated; nature of transition 1 is molecule-dependent, high-temperature transition 2 is observed for all RNAs. **A:** dC $tRNA^{Met}$ transcript (upper profile), wild-type $tRNA^{Met}$ (intermediate profile), and $tRNA^{Met}$ tertiary mutant (A20U, G57A, A60G) (bottom profile) are resolved due to differences in their first melting temperature transition. **B:** dG $tRNA^{Met}$ (upper profile) does not show a low-temperature transition; intermediate and bottom profiles are as in A. **C:** dA $tRNA^{Met}$ transcript. **D:** dU $tRNA^{Met}$ transcript. **E:** Double-substituted dAdU $tRNA^{Met}$ transcript (upper profile) and wild-type transcript (bottom profile). **F:** $tRNA^{Asp}$ transcript (0.2× TBE was used for electrophoresis and no Mg^{2+} has been added during renaturation). **G:** dG $tRNA^{Asp}$ transcript (electrophoresis was performed in 0.5× TB buffer with 5 mM of $MgCl_2$ and renaturation was as for $tRNA^{Met}$; see Materials and Methods). Note the differences in temperature gradients.

taneous RNA cleavages at YpA sequences where Y is either U or C (e.g., Dock-Bregeon & Moras, 1987; Romby et al., 1987). The efficiency of these cuts does not depend on nuclease concentration (not shown). The dA substitution leads to the efficient cuts at the positions 20 and 37 and to increased reactivity at the positions 17, 18, 19, 20, and 21. The dU-substituted transcripts exhibit more efficient cuts at the positions 17, 19, 20, 36, and 47. It is noteworthy that the dA and dU substitutions destabilize the anticodon loop in a different manner, whereas, in the D- and variable loops, they just intensify the patterns typical for the wild-type transcripts. Therefore, it is not surprising that the dAdU substitution destabilizes the anticodon loop significantly, as was evident from the strong cuts appearing at the positions 34, 35, 36, and 37. The most notable change revealed in dC-substituted transcripts is the efficient cleavage at position 48 in the variable loop. For the dG-containing transcript, a shift of the major cut in the variable loop to the position 46, as well as numerous cleavages in the D-stem and loop (positions 18–22), are typical.

Cleavage of $tRNA^{Asp}$ transcript by *N. crassa* nuclease gives one major cut at U35 and minor cuts at positions 36 and 39, which are less than 10-fold efficient

TABLE 1. Transition points for tRNA transcripts containing deoxyribonucleotides.[a]

Transcript		Transition points, °C	
		First	Second
Methionine	wt	43 ± 1	65 ± 1
	dA	38 ± 2	65 ± 1
	dU	38 ± 2	65 ± 1
	dC	32 ± 2	65 ± 1
	dG	—	65 ± 1
	dAdU	—	65 ± 1
Aspartic acid	wt	—	65 ± 1
	dG	—	65 ± 1

[a]Melting of the tertiary and secondary structures of tRNA transcripts containing deoxyribonucleotides.

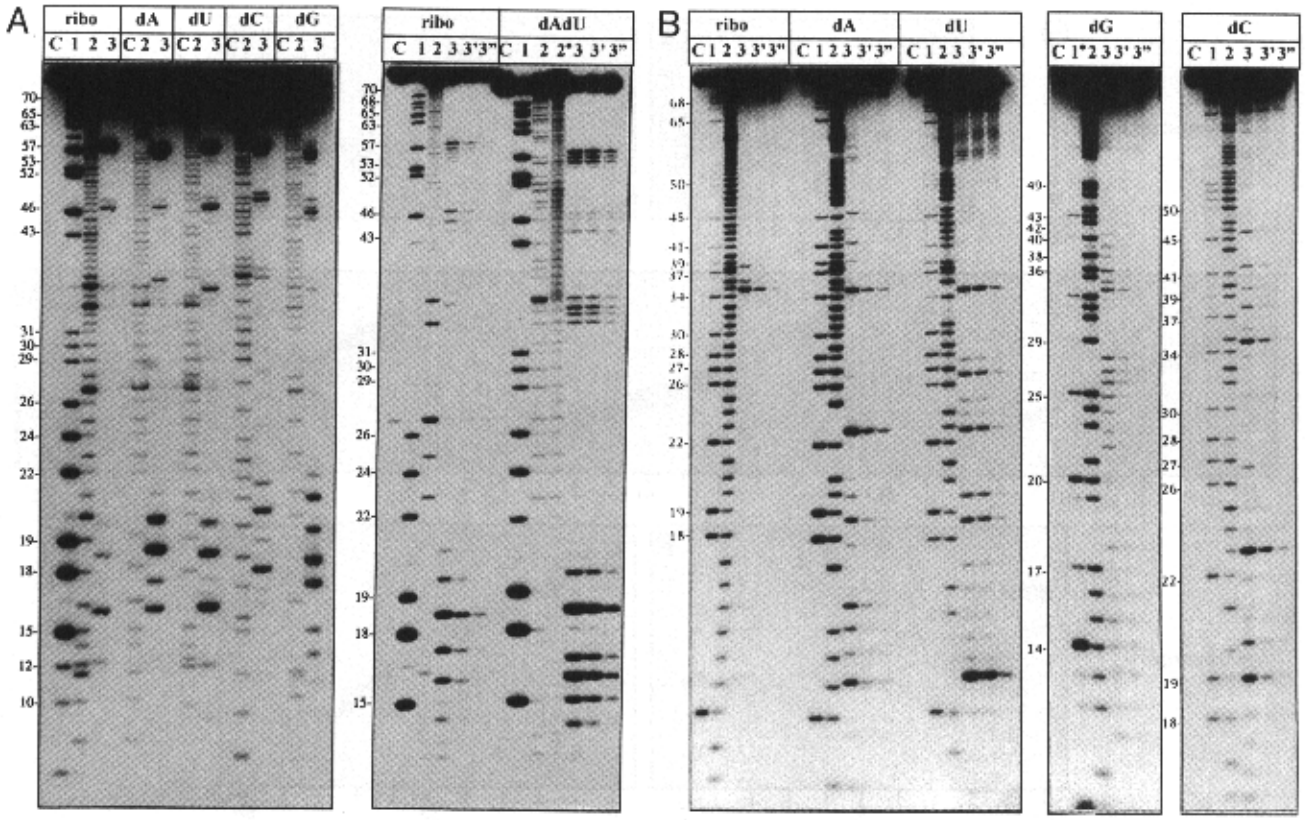

FIGURE 5. Enzymatic probing with *N. crassa* nuclease of $tRNA^{Met}$ (**A**) and $tRNA^{Asp}$ (**B**) deoxyribonucleotide-containing transcripts. Lanes C, control incubations of tRNA transcripts without nuclease; lanes 1, RNase T1 sequencing ladders (lane 1°, we used a T1 digest of dC-tRNA for dG-tRNA); lanes 2, alkaline ladder; lanes 2°, hydroxyl radical ladder; lanes 3, 3', and 3", *N. crassa* nuclease tRNA digests with 0.5, 0.2, and 0.1 U, respectively, of nuclease for 5-min incubations.

(Fig. 5B). Introduction of dA (positions 11–14, 19, 23, and 46) destabilizes the D-stem and interactions between the D- and variable loops. Deoxyuridines confer the same kind of pattern, with some new cuts at positions G27, G28, and U19b. A very strong cut is typical for the position 11. Deoxyguanosine substitution results in structural changes within both single- (positions 14–19, 26, and 34–38) and double- (positions 11–13 and 22–28) stranded regions.

Apparently, the nuclease probing, being a sensitive and selective tool, reveals a complete pattern of structural alterations conferred by deoxyribonucleotide substitutions. It also appears that the lack of some 2'-OH groups could result in overall destabilization of the tertiary structure as seen from increased accessibility of some single-stranded nucleotides visualized for the $tRNA^{Met}$ transcript, as well as affecting double-stranded regions. Destabilization of the D-stem in $tRNA^{Asp}$ seems to be a consequence of removing 2'-OH groups that are participating in tertiary interactions: the presence of dU11, dU12, or dA9 abolishes short-range interactions of 2'-OH groups with 5'-O atoms of the neighboring nucleotide (Westhof et al., 1985).

Aminoacylation properties of $tRNA^{Asp}$ and $tRNA^{Met}$ transcripts containing 2'-deoxyribonucleotides

The results of aminoacylation assays (Table 2) show that deoxyribonucleotide substitutions have different effects on substrate properties of tRNA transcripts. The dA or dU substitutions reduce the aminoacylation efficiency of $tRNA^{Met}$ by about one order of magnitude, whereas the dC or dG substitution and the double-dAdU substitution virtually abolish the aminoacylation capacity of the tRNA transcript. Substitutions of ribonucleotides by dC and dA have almost no influence on the aminoacylation capacity of $tRNA^{Asp}$ transcripts. On the contrary, introduction of dU and dG residues reduces this activity dramatically. This effect, seen both in k_{cat} and K_m, indicates that the affinity between the two macromolecules and the rate of the reaction are disturbed. To understand these effects, participation of 2'-OH groups in tRNA structure and contacts with aminoacyl-tRNA synthetase should be considered.

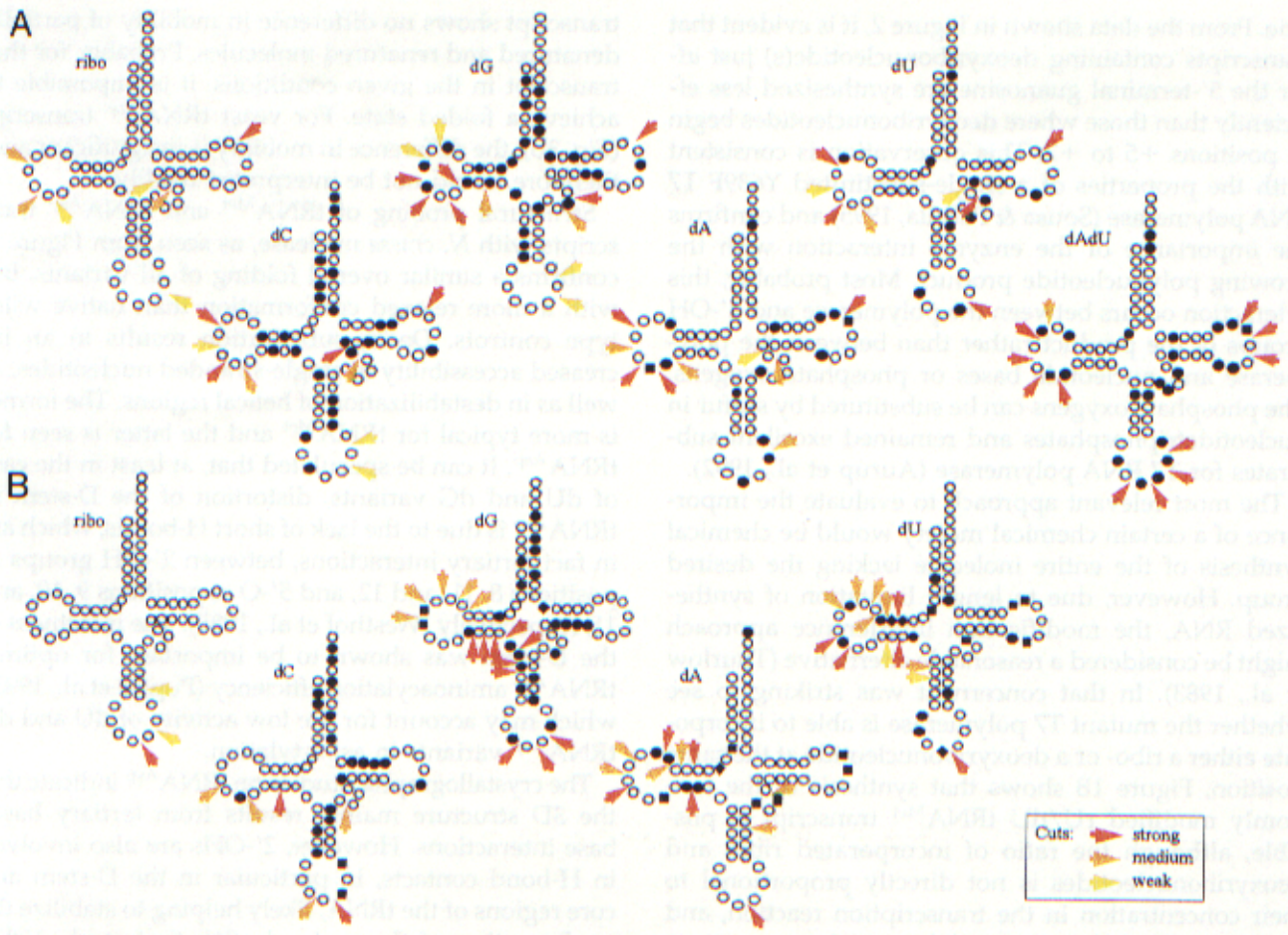

FIGURE 6. Structural *N. crassa* nuclease probing patterns displayed in the cloverleaf representations of $tRNA^{Met}$ (**A**) and $tRNA^{Asp}$ (**B**) wild-type and deoxyribonucleotide-containing transcripts. Open and black circles represent ribo- and deoxyribonucleotides, respectively. Positions and strength of cuts are indicated in color code. In A, the two black squares in the dA and dAdU-$tRNA^{Met}$ folds indicate proximity of 2′-OH of A20 with A59 and of 2′-OH of m^1A58 with A60 (Basavappa & Sigler, 1991); in B, black squares and diamonds show the nucleotides with which those 2′-OH groups form intramolecular H-bonds, with distances 2.6–3.4 Å and <2.6 Å, respectively (Westhof et al., 1985).

DISCUSSION

Mutant T7 RNA polymerase as a tool for RNA structural analysis

The T7 RNA polymerase, after two amino acid substitutions, Y639F and S641A (Kostyuk et al., 1995), acquires the ability to incorporate the deoxyribonucleotides into growing polynucleotide chains. The reduced specificity of the mutant enzyme toward the sugar moiety is not coupled with alteration of the specificity for the bases: the nucleotides are incorporated strictly in a template-directed manner (Fig. 1B). This makes the mutant enzyme a valuable tool for the synthesis of backbone-modified RNA transcripts, which currently are not easily available by chemical synthesis. The yield of deoxyribonucleotide-containing transcription products depends both on the 5′ end sequence of the template and on the chosen deoxyribonucleo-

TABLE 2. Effect of deoxyribonucleotide substitutions on the kinetic parameters of yeast $tRNA^{Met}$ and $tRNA^{Asp}$ transcripts in aminoacylation reaction with cognate aminoacyl-tRNA synthetases.

tRNA variants	Plateau (%)	k_{cat} (s^{-1})	K_m (mM)	Relative k_{cat}/K_m ($s^{-1}\cdot mM^{-1}$)	Loss of efficiency (*x*-fold)
$tRNA^{Asp}$	80	0.690	0.038	1,000	1
dC	57	1.140	0.109	570	1.7
dA	40	0.490	0.093	290	3.4
dU	4	0.006	0.581	0.57	1,750
dG	3	0.001	0.325	0.18	5,500
$tRNA^{Met}$[a]	28	0.3	10	1,000	1
dA[b]	15	0.06	30	70	14.3
dU	22	0.24	83	96	10.4

[a]Molecules with dG, dC, or dAdU are completely inactive.

[b]tRNA has been synthesized without 3′-terminal nucleotide and riboadenosine was added by ATP(CTP):tRNA nucleotidyltransferase treatment (see Materials and Methods). Values of losses of efficiency for duplicates varied by <20%.

tide. From the data shown in Figure 2, it is evident that transcripts containing deoxyribonucleotide(s) just after the 5′-terminal guanosine are synthesized less efficiently than those where deoxyribonucleotides begin at positions +5 to +7. This observation is consistent with the properties of a single-substituted Y639F T7 RNA polymerase (Sousa & Padilla, 1995) and confirms the importance of the enzyme interaction with the growing polynucleotide product. Most probably, this interaction occurs between the polymerase and 2′-OH groups of the product rather than between the polymerase and nucleotide bases or phosphate oxygens. The phosphate oxygens can be substituted by sulfur in nucleotidetriphosphates and remained excellent substrates for T7 RNA polymerase (Aurup et al., 1992).

The most relevant approach to evaluate the importance of a certain chemical moiety would be chemical synthesis of the entire molecule lacking the desired group. However, due to length limitation of synthesized RNA, the modification interference approach might be considered a reasonable alternative (Thurlow et al., 1983). In that concern, it was striking to see whether the mutant T7 polymerase is able to incorporate either a ribo- or a deoxyribonucleotide at the same position. Figure 1B shows that synthesis of the randomly modified rU/dU $tRNA^{Met}$ transcript is possible, although the ratio of incorporated ribo- and deoxyribonucleotides is not directly proportional to their concentration in the transcription reaction, and may depend on the nature of the template.

Structural features of tRNA transcripts with 2′-deoxyribonucleotides

Deoxy-substitution may result in numerous structural changes of tRNA molecule due to the transition of the A conformation of the RNA helices to the DNA-like B conformation, distortion of tertiary interactions, alteration of ion or water binding. Involvement of 2′-hydroxyl groups in direct contacts with aminoacyl-tRNA synthetases can also be important. In order to understand the observed effect of deoxy-substitution on the substrate properties of tRNA transcripts through the RNA structure, we tried to access both the folding of tRNA and the stability of the structure formed.

It appeared that yeast initiator $tRNA^{Met}$ transcript could adopt two conformations that differ in their electrophoretic mobility on a native gel. After renaturation, only the faster migrating conformer remains and may reflect the more compact, presumably native, conformation. We used this phenomenon to monitor the ability of deoxy-containing $tRNA^{Met}$ transcripts to fold into compact (native) conformation. As seen from Figure 3, all $tRNA^{Met}$ variants, except dG-containing ones, behave similarly to full-ribo tRNA transcript, and it may be considered that these molecules presumably possess a similar overall shape. The dG-substituted transcript shows no difference in mobility of partially denatured and renatured molecules. Probably, for that transcript in the given conditions, it is impossible to achieve a folded state. For yeast $tRNA^{Asp}$ transcript (Fig. 3B), the difference in mobility is insignificant and, therefore, could not be interpreted readily.

Structural probing of $tRNA^{Met}$ and $tRNA^{Asp}$ transcripts with *N. crassa* nuclease, as seen from Figure 6, confirms a similar overall folding of all variants, but with a more relaxed conformation than native wild-type controls. Deoxy-substitution results in an increased accessibility of single-stranded nucleotides, as well as in destabilization of helical regions. The former is more typical for $tRNA^{Met}$ and the latter is seen for $tRNA^{Asp}$. It can be speculated that, at least in the case of dU and dG variants, distortion of the D-stem in $tRNA^{Asp}$ is due to the lack of short H-bonds, which are in fact tertiary interactions, between 2′-OH groups in positions 8, 11, and 12, and 5′-O at positions 9, 10, and 11, respectively (Westhof et al., 1985). The intactness of the D-stem was shown to be important for optimal $tRNA^{Asp}$ aminoacylation efficiency (Puglisi et al., 1993), which may account for the low activity of dU and dG $tRNA^{Asp}$ variants in aspartylation.

The crystallographic studies on $tRNA^{Asp}$ indicate that the 3D structure mainly results from tertiary base-base interactions. However, 2′-OHs are also involved in H-bond contacts, in particular in the D-stem and core regions of the tRNA, likely helping to stabilize the conformation of the molecule (Westhof et al., 1985). Altogether, the results presented in this paper indicate that the conformation of tRNA molecules with 2′-OH is indeed altered. Therefore, it can be suggested that this alteration relies on the loss of some of these intramolecular H-bonds involving 2′-OH groups.

Contribution of deoxyriboses in aminoacylation of tRNA transcripts by aspartyl- and methionyl-tRNA synthetases

As a first explanation accounting for the decreased aminoacylation activity of some $tRNA^{Asp}$ and $tRNA^{Met}$ variants containing 2′-deoxyriboses, one may propose an alteration of the active tRNA conformations, due to the destabilizing effect of the loss of some tertiary interactions involving ribose moieties. Such an effect, however, is not the major reason for the decreased aminoacylation capacities observed, because it is well known that tRNA structures with destabilized conformations can still be fully active. This is, for example, the case of $tRNA^{Asp}$ transcripts, as compared to the more stable modified $tRNA^{Asp}$ molecules (Perret et al., 1990a). Moreover, the observed effect is specific for some nucleotides. Although dU and dG $tRNA^{Asp}$ transcripts, as well as dG, dC, and dAdU $tRNA^{Met}$ transcripts, are inactive, variants containing dC or dA for $tRNA^{Asp}$ and dA or dU for $tRNA^{Met}$ are fully active.

This points to specific effects linked to alteration of particular nucleotides in the tRNA. For the methionine system, no precise structural interpretation can be given in the absence of crystallographic knowledge on the structure of the tRNA/synthetase complex. In the aspartate system, where the structure of the complex is known (Ruff et al., 1991; Cavarelli et al., 1993), it is striking that the few H-bond contacts that the synthetase makes with the core of the $tRNA^{Asp}$ involve two H-bonds between 2′-OH groups of the RNA and two amino acids of the protein. Figure 7 shows these contacts between U11 and Asp 210 and between G27 and Glu 202. Interestingly, the variants of $tRNA^{Asp}$ with the strongly reduced aspartylation activity are those where the U and G residues are replaced by dU and dG. Therefore, this interpretation suggests that the loss of activity is due mainly to the loss of either one or the other of these two contacts, although dU- and/or dG-triggered conformational effects contributing to a decreased activity cannot be excluded. The implication of these conclusions is that ribose 11 and ribose 27 are identity elements for aspartylation, but that the identity strength of these elements, as estimated by the loss of catalytic efficiencies of the mutant molecules, might be less important than reflected by the experimental values reported in Table 2. These losses might originate from the dU- and/or dG-triggered overall conformational effects on the $tRNA^{Asp}$ mutants. Thus, the specific replacement of U11 and G27 by dU and dG would mainly lead to a k_{cat} effect on the aminoacylation reaction, as is also the case when mutating aspartate identity bases in yeast $tRNA^{Asp}$ in contact with aspartyl-tRNA synthetase (Giegé et al., 1996).

This structural interpretation could also explain why the dG- and dC-containing $tRNA^{Met}$ variants are inactive, if one assumes an analogous recognition pattern of the tRNA core in tRNA/synthetase complexes with class I synthetases. Indeed, according to the 3D structure of the glutamine complex from *E. coli*, sugar-phosphate backbone contacts of tRNA with the synthetase also comprise residues from the tRNA core (Rould et al., 1991), as in the class II aspartate system. The involved regions in $tRNA^{Met}$ are extremely rich in G and C residues (see Fig. 1). The replacement of such

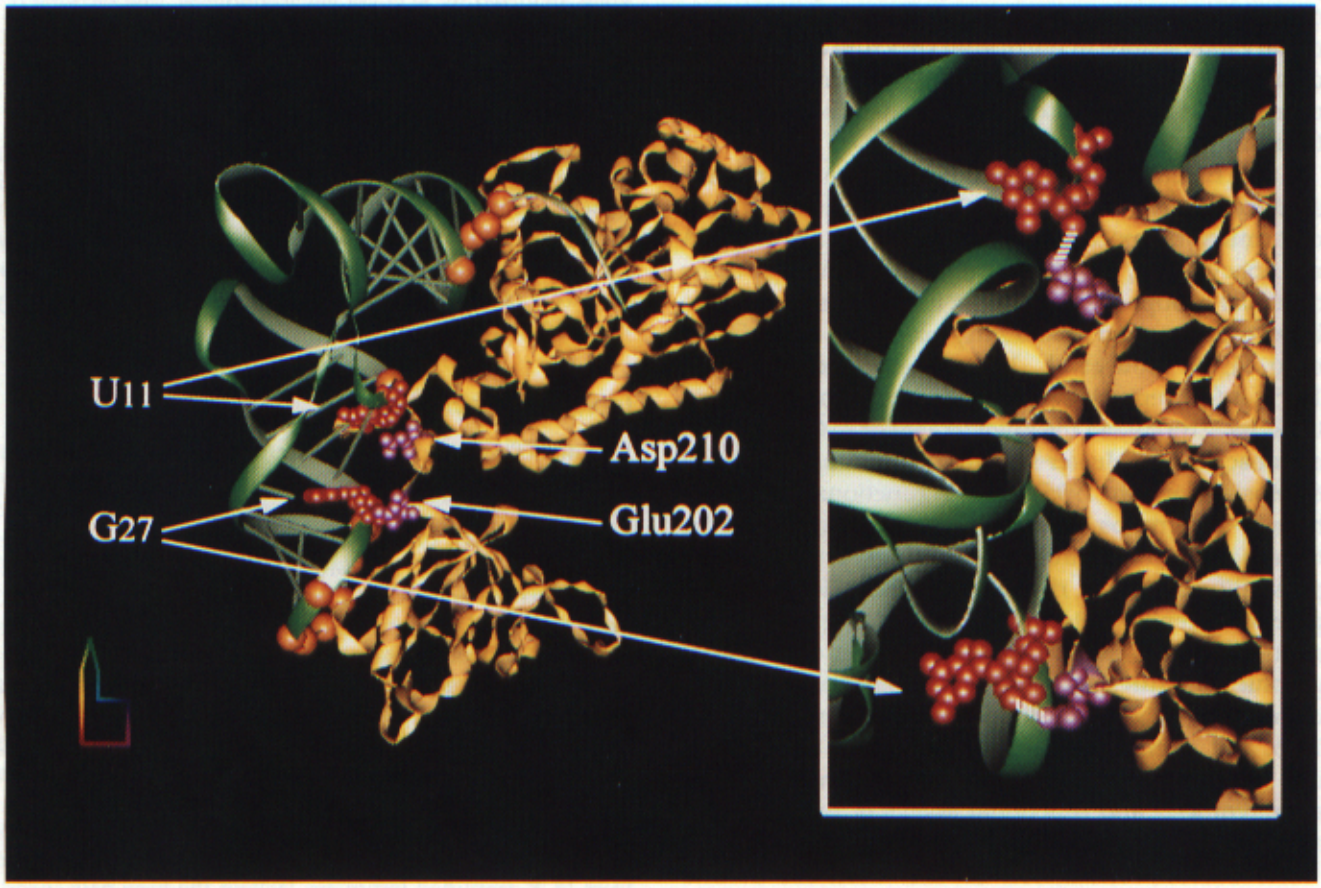

FIGURE 7. Representation of the contacts between yeast aspartyl-tRNA synthetase and its cognate $tRNA^{Asp}$. The 3D structure of one subunit of the dimeric complex is displayed with the protein in yellow and the RNA in green. The tRNA positions in contact with the synthetase (Cavarelli et al., 1993) are indicated in orange balls and in full nucleotide structures for U11 and G27. The two panels at the right emphasize the H-bonding between the 2′-OH groups of U11 and G27 with the Asp 210 and Glu 202 residues of the synthetase. This figure was computed with the software DRAWNA (Massire et al., 1994) using the coordinates from Ruff et al. (1991).

G or C residues by their deoxy-version could account for the inactivity of these molecules. Further experiments using hybrid molecules with deoxy-residues in the sole core region of the tRNA will be needed to test this interpretation explicitly.

Perspectives

As a consequence of the experiments described here, we believe that the use of the T7 polymerase mutant as a tool for structural and functional investigations in the RNA field is widely applicable beyond the limits of tRNA molecules, particularly for single- and double-substituted molecules. Two of the first candidates for further applications might be 5S and 5.8S ribosomal RNAs, due to their reasonable size, well-known structure, and important role played in the ribosomal structure and function. Some other small RNAs are also suitable molecules for this kind of analysis.

As shown here (Table 1), deoxyribo-substitution exhibits entirely different effects on the tertiary and secondary structure of RNAs, severely affecting the former and virtually leaving intact the latter. This property of partially substituted RNAs might be helpful in discriminating the contributions of the tertiary and secondary interactions in the overall structure and function of any RNA. This seems particularly important for numerous cases when other methods are insufficient to distinguish these contributions.

At the functional level, the implications of the present study enlarge our view on the nature of structural determinants specifying RNA functions. For tRNA aminoacylation, architectural features and specific chemical groups carried by the nucleotide bases have been characterized as identity elements (e.g., Giegé et al., 1993; Hou et al., 1993; Musier-Forsyth et al., 1995). A few reports, e.g., for alanine and proline identities, have discussed the involvement of 2′-OH in tRNA aminoacylation (Musier-Forsyth & Schimmel, 1992; Yap & Musier-Forsyth, 1995). Such a functional role of ribose 2′-OH groups is now also strongly suggested for the aspartate and methionine identities. This raises the possibility that such ribose moieties in tRNA can be potential identity determinants specifying aminoacylation efficiency. The fact that the number of crystallographic structures of tRNA/synthetase complexes is increasing (e.g., Arnez & Moras, 1994; Cusack et al., 1996, and references therein) will permit characterizing such riboses and explicitly testing their potency after synthesis and functional assays of the appropriate tRNA transcripts.

The overall conclusions of our work are in line with interpretations given to recent studies on RNA molecules containing modified ribose residues, either Rp-deoxy-phosphorothiates (Hardt et al., 1996), or O-methyl substituted ones (Von Ahsen et al., 1997). In particular, 2′-OH groups in RNase P RNA involved in binding with tRNA (Hardt et al., 1996) or in a tRNA anticodon stem-loop region in binding with ribosome (Von Ahsen et al., 1997) were identified.

MATERIALS AND METHODS

Isolation of a mutant T7 RNA polymerase

T7 phage RNA polymerase containing Y639F and S641A amino acid substitutions has been isolated from the *E. coli* strain BL21 carrying the plasmid pACT7Y639FS641A (Kostyuk et al., 1995). Cells were grown with 34 μg/mL of chloramphenicol at 30 °C to 1 OD at 600 nm, heated to 42 °C in order to inactivate temperature-sensitive Lac repressor, and left at 37 °C for 4 h. Cell lysates and ammonium sulfate fractions were prepared according to Grodberg and Dunn (1988). After overnight dialysis against 20 mM phosphate buffer, pH 7.2, 1 mM EDTA, 1 mM DTT, and 50 mM NaCl, the solution was loaded on a S-Sepharose FF (Pharmacia) column and washed with the same buffer. Elution was performed with the same buffer containing 300 mM NaCl. After 2 h of dialysis against a buffer containing 20 mM Tris-HCl, pH 8.0, 1 mM DTT, 1 mM EDTA, and 50 mM NaCl, the fraction was subjected to a MonoQ 16/10 chromatography (Pharmacia) in a linear 50–500 mM NaCl gradient. Fractions were analyzed by SDS-gel electrophoresis. The enzyme obtained was essentially pure and highly active.

tRNAs and aminoacyl-tRNA synthetases

Unmodified tRNAs were obtained by in vitro transcription of synthetic genes by T7 RNA polymerase. Preparation of methionyl-tRNA synthetase and construction of $tRNA^{Met}$ gene under T7 promoter were described by Senger et al. (1992). Clones of $tRNA^{Asp}$ and pure aspartyl-tRNA synthetase were obtained by standard procedures as described by Perret et al. (1990a,b) and Ng et al. (1996).

In vitro transcription

Plasmid DNA was isolated by centrifugation in CsCl gradient (Sambrook et al., 1989) and digested with *Bst*N I restriction enzyme. Transcription reaction mixture contained 100 mM HEPES, pH 7.5, 20 mM DTT, 1 mM spermidine, 15 mM $MgCl_2$ (or 2.5 mM $MnCl_2$, see Results), 10 mM GMP, 1 mM of rNTP or dNTP, 0.1 mg/mL of plasmid DNA or 0.01 mg/mL of PCR product, 0.1 mg/mL of T7 RNA polymerase, and 100 U/mL of RNase inhibitor (Promega). Reactions (0.5–2 mL) were incubated at 37 °C for 4 h, phenol extracted, ethanol precipitated, and purified to single-nucleotide resolution by 15% polyacrylamide/8 M urea gel electrophoresis followed by electroelution in the Bio-Trap system (Schleicher & Schuell).

In order to preserve the ribonucleotide at the 3′ end of dA-containing $tRNA^{Met}$ transcripts, they were transcribed from PCR-amplified templates lacking the base pair encoding the 3′-terminal nucleotide. For the incorporation of riboadenosine, 50 μM $tRNA^{Met}CpC_{75}$ were incubated in 300 μL of a solution containing 100 mM Tris-HCl, pH 9.0, 100 mM KCl, 10 mM $MgCl_2$, 1 mM DTT, and 3 mM ATP with 50 nM ATP(CTP):tRNA nucleotidyltranferase for 5 h at 25 °C. The

pH of the mixture was lowered by adding 30 μL of 2 M sodium acetate buffer, pH 4.5. After addition of 300 μL of water, the solution was applied to a 0.5 cm × 1 cm column of DEAE FastFlow (Pharmacia), equilibrated with 10 mM $MgCl_2$, 200 mM NaCl in 20 mM sodium acetate buffer, pH 5.2. Excess nucleoside-5'-triphosphates and enzyme were washed off with the same buffer. tRNA was eluted with the same buffer containing 1 M NaCl and ethanol precipitated.

Structural probing with *N. crassa* nuclease

tRNA was dephosphorylated by bacterial alkaline phosphatase and 5' labeled by T4 polynucleotide kinase in the presence of [γ-^{32}P] ATP (NEN) according to the standard protocols. tRNA has been renatured in the same way as for aminoacylation. Reaction mixture containing 20 mM HEPES, pH 7.5, 5 mM $MgCl_2$, 150 mM NaCl, 1 mg of total yeast tRNA, 5'-labeled tRNA (50,000 cpm), 0.1–0.5 U of *N. crassa* nuclease (Boehringer-Mannheim, Meylan) was incubated for 5 min at 25 °C, phenol extracted, ethanol precipitated, and analyzed in 15% polyacrylamide/8 M urea gel. The digestion patterns were compared with T1 RNase, alkaline, or Fe^{2+}-EDTA ladders (see below). Alkaline ladders have been generated by incubation of 5'-labeled tRNA (100,000 cpm) in 5 μL of 50 mM $NaHCO_3$, pH 9.0, at 95 °C for 3 min. After cooling the reaction mixture on ice, 5 μL of deionized formamide was added. Hydroxy radical ladders were obtained according to Hüttenhofer and Noller (1992), with minor modifications. 5'-Labeled RNA (100,000 cpm) was renatured as described above in a total volume of 20 μL and mixed with 1 μL of 250 mM DTT, 1 μL of $Fe(NH_4)_2(SO_4)_2$,$6H_2O$ (20 mg/mL), and 1 μL of H_2O_2. Reaction was performed at 20 °C for 1–5 min and stopped by ethanol precipitation. Patterns obtained in 7 M urea, instead of Mg^{2-}-containing buffer, were considered as reflecting the unfolded RNA state.

Native gel electrophoresis

Native gel electrophoresis has been run in 10% acrylamide gel with 45 mM Tris-borate buffer, pH 8.3, and 5 mM $MgCl_2$ at 4 °C for 2–6 h. RNA samples were loaded either without any renaturation or renatured as for footprinting experiments. Before loading, glycerol was added to 10% final concentration and samples were incubated on ice for 5 min. After electrophoresis, the gel was dried and exposed to the X-ray film.

Temperature-gradient gel electrophoresis

Thermal denaturation profiles were determined by TGGE [for a review, see Riesner et al. (1991)] using DIAGEN-TGGE System (DIAGEN, Hilden, Germany). The linear temperature gradient was established perpendicular to the direction of electrophoresis using two thermostatic baths. The RNA sample was prepared as for native gel electrophoresis, loaded in 100 μL on the broad slot, and run for 2 h at 250 V. Gels contained 12% polyacrylamide (acrylamide/bisacrylamide ratio was 29/1) and 0.5× Tris-Borate buffer. RNA was visualized by X-ray autoradiography or by silver staining according to manufacturer's instruction. Two or more RNAs were analyzed on one gel. Independent experiments with unlabeled and labeled RNA, and both silver staining and X-radiography, were used to verify the origin of each band on the gel.

Amino acid acceptor activity of tRNA transcripts

Aminoacylation was performed at 25 °C in 100-μL reaction mixture containing 20 mM HEPES, pH 7.5, 10 mM $MgCl_2$, 1 mM DTT, 2 mM ATP, 0.1 mM methionine or 0.05 mM aspartic acid, and 5–100 nM of pure aminoacyl-tRNA synthetase. tRNA concentration ranged from 0.1 to 80 μM. [^{35}S] methionine (specific activity 500 cpm/pmol) and [^{3}H] aspartic acid (specific activity 3,000 cpm/pmol) have been used. Aliquots were taken at 0.5–1-min intervals, spotted on Whatman 3MM pads pre-soaked in 10% TCA, and rinsed 5 times with 5% TCA. Prior to aminoacylation, tRNA transcripts were heated in water at 90 °C for 1 min, left at room temperature for 5 min, and then incubated 5 min with the reaction buffer at 25 °C.

ACKNOWLEDGMENTS

This work was supported by grants from the Centre National de la Recherche Scientifique (CNRS) and the Université Louis Pasteur (ULP), Strasbourg. We thank Mark Helm for help during the TGGE experiments and Catherine Florentz for fruitful discussions. L.K. acknowledges the support from Volkswagen (a "Transfer RNA folding" project). R.A. was supported by an EMBO short-term fellowship. D.K. and S.K. were supported by the Howard Hughes Medical Institute (project 75195-545003).

Received March 10, 1997; returned for revision April 30, 1997; revised manuscript received May 27, 1997

REFERENCES

Aphasizhev R, Senger B, Fasiolo F. 1997. Importance of structural features for $tRNA^{Met}$ identity. *RNA* 3:489–497.

Arnez JG, Moras D. 1994. Aminoacyl-tRNA synthetase-tRNA recognition. In: Nagai K, Mattaj IW, eds. *RNA–protein interactions*. Oxford: IRL Press. pp 52–81.

Aurup H, Williams DM, Eckstein F. 1992. 2'-Fluoro- and 2'-amino-2'-deoxynucleoside 5'-triphosphates as substrates for T7 RNA polymerase. *Biochemistry* 31:9636–9641.

Basavappa R, Sigler PB. 1991. The 3 Å crystal structure of yeast initiator tRNA: Functional implications in initiator/elongator discrimination. *EMBO J* 10:3105–3111.

Biou V, Yaremchuk A, Tukalo M, Cusack S. 1994. The 2.9 Å crystal structure of *T. thermophilus* seryl-tRNA synthetase complexed with $tRNA^{Ser}$. *Science* 263:1404–1410.

Cavarelli J, Rees B, Ruff M, Thierry JC, Moras D. 1993. Yeast $tRNA^{Asp}$ recognition by its cognate class II aminoacyl-tRNA synthetase. *Nature* 362:181–184.

Conrad F, Hanne A, Gaur RK, Krupp G. 1995. Enzymatic synthesis of 2'-modified nucleic acids: Identification of important phosphate and ribose moieties in RNase P substrates. *Nucleic Acids Res* 23:1845–1853.

Cusack S, Yaremchuk A, Tukalo M. 1996. The crystal structures of *T. thermophilus* lysyl-tRNA synthetase complexed with *E. coli* $tRNA^{Lys}$ and a *T. thermophilus* $tRNA^{Lys}$ transcript: Anticodon recognition and conformational changes upon binding of a lysyl-adenylate analogue. *EMBO J* 15:6321–6334.

Dock-Bregeon AC, Moras D. 1987. Conformational changes and dynamics of tRNAs: Evidence from hydrolysis patterns. *Cold Spring Harbor Symp Quant Biol 52*:113–121.

Fraser MJ. 1980. Purification and properties of *Neurospora crassa* endoexonuclease, an enzyme which can be converted to a single-strand specific endonuclease. *Methods Enzymol 65*:255–263.

Gangloff J, Keith G, Ebel JP, Dirheimer G. 1971. Structure of aspartate tRNA from brewer's yeast. *Nature New Biol 230*:125–127.

Giegé R, Florentz C, Kern D, Gangloff J, Eriani G, Moras D. 1996. Aspartate identity of transfer RNAs. *Biochimie 78*:605–623.

Giegé R, Puglisi JD, Florentz C. 1993. tRNA structure and aminoacylation efficiency. *Prog Nucleic Acids Res Mol Biol 45*:129–206.

Grodberg J, Dunn JJ. 1988. *ompT* encodes the *Escherichia coli* outer membrane protease that cleaves T7 RNA polymerase during purification. *J Bacteriol 170*:1245–1253.

Hardt WD, Erdmann VA, Hartmann RK. 1996. Rp-deoxy-phosphorothioate modification interference experiments identify 2'-OH groups of RNase P RNA that are crucial to tRNA binding. *RNA 2*:1189–1198.

Hou YM, Westhof E, Giegé R. 1993. An unusual RNA tertiary interaction has a role for the specific aminoacylation of a transfer RNA. *Proc Natl Acad Sci USA 90*:6776–6780.

Hüttenhofer A, Noller HF. 1992. Hydroxyl radical cleavage of tRNA in the ribosomal P site. *Proc Natl Acad Sci USA 89*:7851–7855.

Khan AS, Roe BA. 1988. Aminoacylation of synthetic DNAs corresponding to *Escherichia coli* phenylalanine and lysine tRNAs. *Science 241*:74–79.

Kostyuk DA, Dragan SM, Lyakhov DL, Rechinsky VO, Tunitskaya VL, Chernov BK, Kochetkov SN. 1995. Mutants of T7 RNA polymerase that are able to synthesize both RNA and DNA. *FEBS Lett 369*:165–168.

Massire C, Gaspin C, Westhof E. 1994. DRAWNA: A program for drawing schematic views of nucleic acids. *J Mol Graphics 12*:201–206.

Moore MJ, Sharp PA. 1992. Site-specific modification of pre-mRNA: The 2'-hydroxyl groups at the splice sites. *Science 256*:992–997.

Musier-Forsyth K, Schimmel P. 1992. Functional contacts of a transfer RNA synthetase with 2'-hydroxyl groups in the RNA minor groove. *Nature 357*:513–515.

Musier-Forsyth K, Shi JP, Henderson B, Bald R, Fürste JP, Erdmann VA, Schimmel P. 1995. Base-analog-induced aminoacylation of an RNA helix by a tRNA synthetase. *J Am Chem Soc 117*:7253–7254.

Ng J, Lorber B, Witz J, Théobald-Dietrich A, Kern D, Giegé R. 1996. The crystallization of macromolecules from precipitates: Evidence for Ostwald ripening. *J Crystal Growth 168*:50–62.

Paquette J, Nicoghosian K, Qi GR, Beauchemin N, Cedergren R. 1990. The conformation of single-stranded nucleic acids tDNA versus tRNA. *Eur J Biochem 189*:259–265.

Perret V, Garcia A, Grosjean H, Ebel JP, Florentz C, Giegé R. 1990a. Relaxation of transfer RNA specificity by removal of modified nucleotides. *Nature 344*:787–789.

Perret V, Garcia A, Puglisi JD, Grosjean H, Ebel JP, Florentz C, Giegé R. 1990b. Conformation in solution of yeast $tRNA^{Asp}$ transcripts deprived of modified nucleotides. *Biochimie 72*:735–744.

Puglisi JD, Pütz J, Florentz C, Giegé R. 1993. Influence of tRNA tertiary structure and stability on aminoacylation by yeast aspartyl-tRNA synthetase. *Nucleic Acids Res 21*:41–49.

Pütz J, Puglisi JD, Florentz C, Giegé R. 1991. Identity elements for specific aminoacylation of yeast $tRNA^{Asp}$ by cognate aspartyl-tRNA synthetase. *Science 252*:1696–1699.

Pyle AM, Cech TR. 1991. Ribozyme recognition of RNA by tertiary interactions with specific ribose 2'-OH groups. *Nature 350*:628–631.

Pyle AM, Murphy FL, Cech TR. 1992. RNA substrate binding site in the catalytic core of the *Tetrahymena* ribozyme. *Nature 358*:123–128.

Riesner D, Henco K, Steger G. 1991. Temperature-gradient gel electrophoresis: A method for the analysis of conformational transitions and mutations in nucleic acids and proteins. In: Chrambach A, Dunn MJ, Radola BJ, eds. *Advances in Electrophoresis*, 4. Weinheim, Germany: VCH. pp 169–249.

Romby P, Moras D, Dumas P, Ebel JP, Giegé R. 1987. Comparison of the tertiary structure of yeast $tRNA^{Asp}$ and $tRNA^{Phe}$ in solution. Chemical modification study of the bases. *J Mol Biol 195*:193–204.

Rould MA, Perona JJ, Söll D, Steitz TA. 1989. Structure of *E. coli* glutaminyl-tRNA synthetase complexed with $tRNA^{Gln}$ and ATP at 2.8 Å resolution. *Science 246*:1135–1142.

Rould MA, Perona JJ, Steitz TA. 1991. Structural basis of anticodon loop recognition by glutaminyl-tRNA synthetase. *Nature 352*:213–218.

Ruff M, Krishnaswamy S, Boeglin M, Poterszman A, Mitschler A, Podjarny A, Rees B, Thierry JC, Moras D. 1991. Class II aminoacyl transfer RNA synthetases: Crystal structure of yeast aspartyl-tRNA synthetase complexed with $tRNA^{Asp}$. *Science 252*:1682–1689.

Sambrook J, Fritsch EF, Maniatis T. 1989. *Molecular cloning: A laboratory manual*. Cold Spring Harbor, New York: Cold Spring Harbor Laboratory Press.

Senger B, Aphasizhev R, Walter P, Fasiolo F. 1995. The presence of a D-stem but not a T-stem is essential for triggering aminoacylation upon anticodon binding in yeast methionine tRNA. *J Mol Biol 249*:45–48.

Senger B, Despons L, Walter P, Fasiolo F. 1992. The anticodon triplet is not sufficient to confer methionine acceptance to a transfer RNA. *Proc Natl Acad Sci USA 89*:10768–10771.

Seong BL, RajBhandary UL. 1987. *Escherichia coli* formylmethionine tRNA: Mutations in the GGG/CCC sequence conserved in anticodon stem of initiator tRNAs affect initiation of protein synthesis and conformation of anticodon loop. *Proc Natl Acad Sci USA 84*:334–338.

Simsek M, RajBhandary UL. 1972. The primary structure of yeast initiator transfer RNA. *Biochem Biophys Res Commun 49*:508–515.

Sousa R, Padilla R. 1995. A mutant T7 RNA polymerase as a DNA polymerase. *EMBO J 14*:4609–4621.

Thurlow DL, Ehresmann C, Ehresmann B. 1983. Nucleotides in 16S rRNA that are required in unmodified form for features recognized by ribosomal protein S8. *Nucleic Acids Res 11*:6787–6802.

Von Ahsen U, Green R, Schroeder R, Noller HF. 1997. Identification of 2'-hydroxyl groups required for interaction of a tRNA anticodon stem-loop region with the ribosome. *RNA 3*:49–56.

Westhof E, Dumas P, Moras D. 1985. Crystallographic refinement of yeast aspartic acid transfer RNA. *J Mol Biol 184*:119–145.

Williams DM, Pieken WA, Eckstein F. 1992. Function of specific 2'-hydroxyl groups of guanosines in a hammerhead ribozyme probed by 2' modifications. *Proc Natl Acad Sci USA 89*:918–921.

Yap LP, Musier-Forsyth K. 1995. Transfer RNA aminoacylation: Identification of a critical ribose 2'-hydroxyl-base interaction. *RNA 1*:418–424.